Jurnal Ilmu Fisika
Vol. 17, No. 2, September 2025, pp. 135–145
ISSN: 1979-4657 (Print); 2614-7386 (Online)
https://doi.org/ 10.25077/jif.17.2.135-145.2025

Jurnal Ilmu Fisika
Open Access

Influence of Binder Type on the Physical, Magnetic, and Mechanical Properties of Sintered Barium Hexaferrite: A Comparison between Polyvinyl Alcohol and Silicone Rubber

Wahyu Solafide Sipahutar, Gustya Salma Putrie, Faiza Armalia Putri, Abi Farhan, M Hafid, Eka Nurfani, Nur Istiqomah Khamidy, Aditya Rianjanu

The Department of Materials Engineering, Institut Teknologi Sumatera, Lampung Selatan, 35365, Indonesia

Article Info

Article History:

Received April 21, 2025
Revised May 21, 2025
Accepted May 29, 2025
Published online May 31, 2025

Keywords:

barium hexaferrite
polyvinyl alcohol
silicone rubber
magnetic properties
sintering

Corresponding Author:

Wahyu Solafide Sipahutar,
Email:
Wahyu.sipahutar@mt.itera.ac.id

ABSTRACT

This study explores the impact of binder types—polyvinyl alcohol (PVA) and silicone rubber (SR)—on the physical, magnetic, and mechanical properties of barium hexaferrite ($BaFe_{12}O_{19}$), synthesized via mechanical alloying and sintered at 1100°C. SEM-EDX confirmed the formation of $BaFe_{12}O_{19}$ with an average particle size of around 0.7 µm. VSM results showed a saturation magnetization (M_s) of 71.17 emu/g, remanent magnetization (M_r) of 47.8 emu/g, and coercivity (H_c) of 0.33 T. The addition of PVA reduced density (3.13–3.07 g/cm³), increased porosity (17.72%–18.47%), and decreased magnetization (0.93–0.80 mT). In contrast, SR enhanced densification, leading to higher density (3.65–3.57 g/cm³), lower porosity (6.95%–7.51%), and significantly higher hardness (232.9–438.92 HV). SR also improved mechanical strength, while PVA proved more effective in reducing shrinkage and improving magnetization. These results underscore the significant role of binder type and concentration in optimizing the properties of sintered barium hexaferrite, with SR excelling in mechanical strength and PVA in magnetization.

1. INTRODUCTION

Global demand for permanent magnets has significantly increased in recent years due to the growing number of applications derived from permanent magnets (Ghorbani et al., 2025; Hirosawa et al., 2017; Islam et al., 2024). The application of permanent magnets is most found in the industrial sector, as well as in electronics, automotive, and even household industries. Due to the increasing number of applications and roles of permanent magnets, the demand for their properties and performance is also rising. There is a growing need for science and innovation in the development of magnetic materials to meet the broader demands of users. One of the recent applications of innovation is the use of electric motors and renewable energy. Thus, magnets also support the utilisation of materials to promote environmental friendliness.

Barium hexaferrite ($BaFe_{12}O_{19}$) is one type of permanent magnet that has advantages such as good magnetic properties, resistance to demagnetisation, and good thermal resistance, making barium hexaferrite often used for various applications and continuously developed (Darmawan et al., 2025; Martínez-Hernando et al., 2023). Therefore, the continuous innovation of barium hexaferrite is crucial to expand the applications of permanent magnets (Hassan et al., 2024; Koutzarova et al., 2013; Rusianto et al., 2015; Thongsamrit et al., 2022). The increasing demand for innovative materials in technology

highlights the important role that barium hexaferrite will play in shaping the future of various electronic and energy-related industries.

Although barium hexaferrite has several advantages, it still faces some challenges that need to be addressed to further improve its performance. One of the aspects to consider is its production technique. The most influential processing technique is how sintered materials often have low density, which is caused by high porosity during the sintering and compaction stages (An et al., 2014; Vinnik et al., 2017). Using additives that aid the sintering process and adjusting the temperature and sintering time can significantly improve the density and magnetic properties of the material, which can help address this issue. This manufacturing technique can also contribute to an improved microstructure of barium hexaferrite, which is closely linked to its physical properties. Porosity, for instance, influences the mechanical strength and magnetic behaviour of the final product. However, uneven microstructures often develop during the fabrication process, resulting in variations in coercivity, remanence, and other magnetic properties (Breitwieser et al., 2017; Cui et al., 2022). To address these challenges, optimizing synthesis and post-synthesis treatment parameters is essential.

Careful control of heat treatment and cooling rates can promote the development of a more homogeneous microstructure, ultimately enhancing the magnetic performance and stability of barium hexaferrite. Moreover, insufficient packing and poor particle adhesion commonly lead to reduced strength of green magnetic pellets during the forming stage. To improve particle cohesion and printability prior to sintering, binders are often incorporated during this process. However, limited research has explored how different types of binders influence the mechanical, magnetic, and physical properties of sintered barium hexaferrite. Therefore, a deeper understanding of binder behaviour during manufacturing is critical for advancing techniques aimed at producing high-quality permanent magnets (Wagner et al., 2023). This knowledge is crucial to optimising the production of barium hexaferrite and enhancing its performance for various applications. Further studies will focus on the methodical analysis of various types of binders and how they relate to the magnetic characteristics of the final product.

The selection of binders during the forming stage is a critical factor in the production of ceramic and magnetic materials such as barium hexaferrite, as it significantly influences the quality of the green body and the resulting microstructure after sintering (Ghorbani et al., 2025; Sipahutar & Muljadi, 2021). Among the various binders, polyvinyl alcohol (PVA) is the most commonly used due to its affordability, water solubility, and clean-burning characteristics during thermal treatment. PVA not only improves the mechanical cohesion and structural integrity of the green body but also leaves minimal residue after sintering. In addition to PVA, alternative binders such as silicone rubber (SR) offer several advantages, including high flexibility, chemical inertness, and excellent thermal stability. Despite these benefits, SR is not widely applied in the processing of ferrite magnets (Owens et al., 2016). The type of binder used can significantly influence pore evolution, matrix flexibility, and chemical interactions during high-temperature sintering, ultimately affecting the mechanical and magnetic properties of the final product.

While extensive research has been conducted on traditional organic binders such as PVA and PEG, comparative studies involving silicone-based adhesives remain limited—particularly for strong magnetic ceramics like barium hexaferrite. A direct comparison between organic (e.g., PVA) and inorganic (e.g., silicone rubber) binders is essential for understanding their roles in tailoring the microstructure and enhancing the functional properties of sintered ferrite materials (Idayanti et al., 2017; Idayanti & Manaf, 2018). PVA is well known for its flexibility, water solubility, and film-forming ability, all of which contribute to improved mechanical properties in composites (Banerjee et al., 2019; Ridwan et al., 2011). Meanwhile, silicone rubber exhibits outstanding thermal stability, elasticity, and chemical resistance, which can extend the performance and lifespan of barium hexaferrite-based technologies, as reported in previous studies (Hassan et al., 2024; Idayanti & Manaf, 2018; Thongsamrit et al., 2022).

The primary objective of this research is to investigate how variations in binder type—specifically PVA and silicone rubber—affect the physical, magnetic, and mechanical properties of sintered barium hexaferrite. Key parameters examined include density, porosity, surface morphology, remanence, coercivity, saturation magnetization, and material hardness. This study also aims to establish a clear relationship between binder type, microstructural evolution, and the overall performance of the

material following high-temperature sintering. The findings are expected to provide novel insights into the role of binders in optimizing magnetic ceramics, as well as valuable experimental references for the development of high-performance sintered magnets. Finally, this research contributes to the advancement of scalable and data-informed binder processing strategies for industrial applications.

2. METHOD

Barium hexaferrite powder was synthesized using the mechanical alloying method by mixing $BaCO_3$ and Fe_2O_3 in a molar ratio of 1:6. The mixture is then placed into an mechanical milling jar along with steel balls and undergoes a milling process for 12 hours. After the milling process, the resulting powder is sieved using a 300-mesh sieve. At this stage, characterization is performed using scanning electron microscopy (SEM) to examine the surface morphology and ensure the formation of a hexagonal barium hexaferrite structure. Additionally, Vibrating Sample Magnetometry (VSM) is used to measure magnetic properties such as remanent magnetization (M_r), coercivity (H_c), and saturation magnetization (M_s) to ensure these values are close to the results of previous studies. This characterization ensures that the $BaFe_{12}O_{19}$ phase has formed before mixing with the binder. After checking the structure and magnetic properties, 4 grams of the sifted powder were mixed with PVA binder or SR at two different amounts, 5% and 10% by weight, to see how changing the binder concentration affects the material properties. This homogeneous mixture was then shaped and compacted using a hydraulic press with a pressure of 3000 psi to form magnetic pellets.

The formed pellets are then sintered at a temperature of 1100 °C for 1 hour to obtain the optimal crystalline phase of $BaFe_{12}O_{19}$. The sintered samples were subsequently reanalyzed using SEM for surface morphology and microstructure evaluation. The measurement of strong magnetic fields was conducted using a Gauss meter. Additionally, density and porosity are determined according to ASTM C20 standards, while shrinkage is calculated by comparing the mass before and after sintering. The mechanical strength was tested using a Universal Vickers Hardness Tester according to ASTM E384. Each treatment variation in this experimental is conducted with a minimum of three repetitions for each sample to obtain a representative average value. The measurement results are presented along with the standard deviation as indicators of data variation and consistency. This detailed analysis helps us understand how changes in the binder affect the physical, magnetic, and mechanical properties of sintered barium hexaferrite.

3. RESULTS AND DISCUSSION

3.1 Microstructure Analysis

Figure 1 presents Scanning Electron Microscope (SEM) images captured at magnifications of 10,000x and 25,000x, clearly revealing the characteristic hexagonal morphology of barium hexaferrite. This distinctive hexagonal structure is a definitive indicator that the synthesized material is indeed $BaFe_{12}O_{19}$ (Kanagesan et al., 2015). The SEM analysis shows an average particle size of approximately 0.7 µm, demonstrating that the milling process effectively produced particles that are both small and relatively uniform. While there is some variability in particle size, with certain particles being larger or smaller than the average, the overall distribution remains homogeneous (Madavali et al., 2021). Moreover, the images reveal particle aggregation, where individual particles adhere and cluster together. Such agglomeration can significantly influence material properties, including sintering density and magnetic behaviour. The sintering process, conducted at 1100 °C, contributes to reducing porosity and enhancing the material's density, as evidenced by the well-integrated particles seen in the SEM images. However, this high-temperature treatment may also promote particle agglomeration, which is visually apparent (Mahmood & Bsoul, 2012).

The Energy Dispersive X-ray Spectroscopy (EDX) analysis, supported by the compositional data, confirms the presence of the key elemental constituents of barium hexaferrite: barium (Ba), iron (Fe), and oxygen (O). The composition is dominated by iron and barium, consistent with the expected stoichiometry of $BaFe_{12}O_{19,}$ while oxygen plays an essential role in maintaining the crystal lattice

(Madavali et al., 2021; Mahmood & Bsoul, 2012). The measured oxygen content is slightly lower than the theoretical value, which can be attributed to limitations in EDX detection accuracy for light elements and potential oxygen loss during the high-temperature sintering process. Overall, the elemental composition closely aligns with the ideal formula for barium hexaferrite, providing strong evidence that the synthesis and sintering procedures were successful in producing a phase-pure material with the desired structural and compositional characteristics.

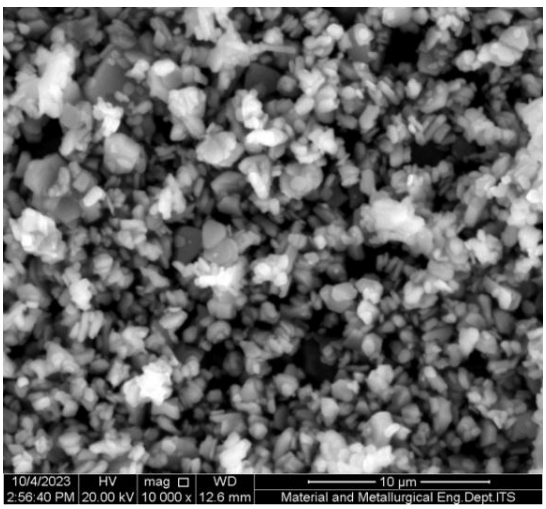

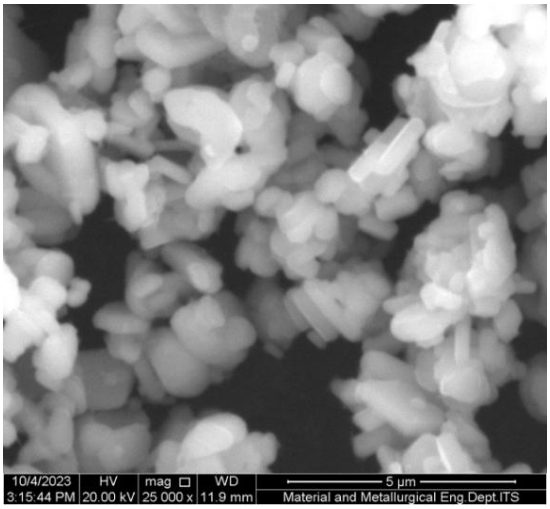

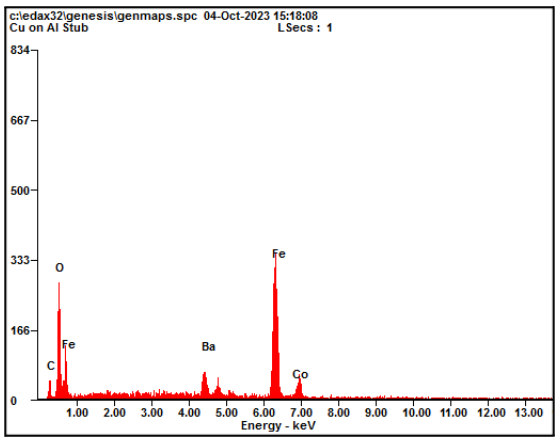

Element	Wt%	At%
CK	04.56	14.04
OK	17.24	39.81
BaL	13.98	03.76
FeK	61.26	40.53
CoK	02.96	01.85
Matrix	Correction	ZAF

Figure 1. SEM micrograph and EDX barium hexaferrite powder sinter at 1100°C.

3.2 Magnet Properties of VSM Barium Hexaferrite

Figure 2 shows the magnetic hysteresis curve of barium hexaferrite synthesized via mechanical alloying and sintered at 1100 °C, measured using Vibrating Sample Magnetometry (VSM). The magnetization curve reveals a M_s of 71.17 emu/g, a M_r of 47.8 emu/g, and a H_c of 0.33 T. These values closely match those reported in previous studies on $BaFe_{12}O_{19}$, such as Gutfleisch et al. (2011), who observed M_s values around 70–75 emu/g and H_c between 0.3 and 0.4 T, and by P. Singh et al. (2014), who reported similar magnetic characteristics. This consistency suggests that a well-formed hexagonal magneto plumbite phase was achieved, with minimal secondary phases or microstructural defects that could compromise magnetic performance. The high remanence and coercivity indicate strong magnetic stability, making this material highly suitable for permanent magnet applications. These findings also confirm that the processing conditions used—particularly the sintering temperature of 1100 °C—are effective in producing high-quality magnetic ceramics. Having established these intrinsic magnetic properties, the next step in this study is to investigate how variations in binder type and concentration,

specifically PVA and SR, affect the physical, magnetic, and mechanical properties of the sintered barium hexaferrite. Understanding the role of the binder is essential for optimizing both the microstructure and the final magnetic performance.

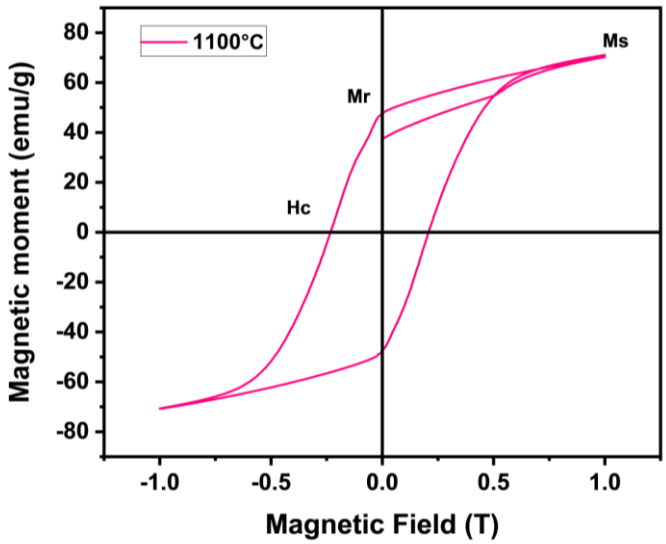

Figure 2. The VSM graph of barium hexaferrite sintering at 1100°C.

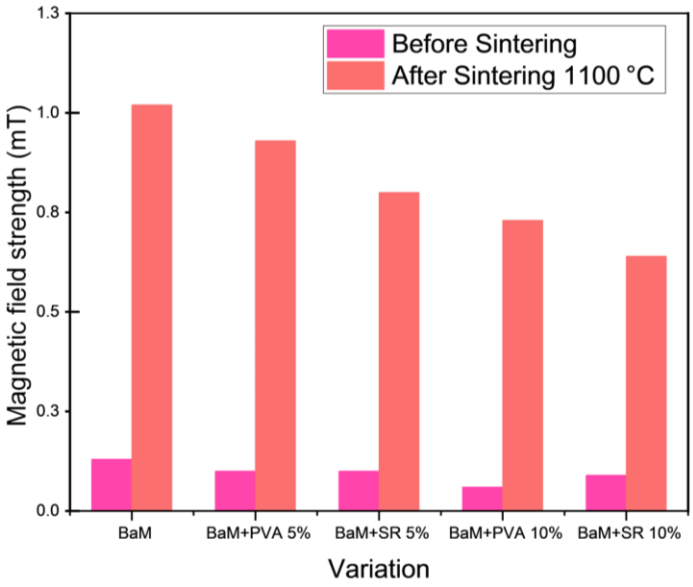

Figure 3. Magnetic field strength (in millitesla, mT) of barium hexaferrite samples before and after sintering, measured using a gaussmeter.

Figure 3 shows big differences in the magnetic field strengths measured with gaussmeters between samples of PVA and SR binder at different concentrations. It recorded non-adhesive barium hexaferrite magnetization at 0.13 mT before the sintering process. The magnetization increased significantly after sintering, reaching 1.02 mT. After adding 5% PVA adhesive to hexaferrite barium, the first magnetization increased to 0.93 mT after sintering. For barium hexaferrite with SR 5%, the first magnetization was also 0.10 mT, but it increased only to 0.80 mT after sintering. Adding PVA to a binder concentration of 10% produced a first magnetization of 0.06 mT, which increased to 0.73 mT after sintering. By contrast, the addition of SR produced an initial magnetization of 0.09 mT, which

increased to 0.64 mT after sintering. These findings indicate that, at both 5% and 10% concentrations, PVA binders tend to result in a greater enhancement of magnetization compared to SR.

The sintering process promotes the growth of larger and better-defined crystals. This increase in crystallinity reduces grain boundaries and structural imperfections, thereby improving magnetic properties by minimizing domain wall pinning. Sintering also facilitates better magnetic domain alignment (El Shater et al., 2018; Manglam et al., 2021; Wang et al., 2010a; Zou et al., 2023). However, the greatest increase in magnetization was observed in the pure barium hexaferrite sample without any binder. This is likely because the absence of binder eliminates the possibility of residual binder decomposition products remaining in the structure after sintering. Residuals from binder burnout can introduce impurities or porosity, which may hinder magnetic domain alignment and reduce magnetic performance (Liu et al., 2013). Therefore, the pure sample can achieve a more complete enhancement of its magnetic properties due to cleaner microstructural development and fewer non-magnetic inclusions. This result suggests that the presence of either PVA or SR binders may slightly inhibit the full enhancement of magnetic properties after sintering.

3.3 Physical Properties

Table 1 shows the density and porosity measurements of barium hexaferrite samples prepared with different binders PVA and SR—at varying concentrations. As a baseline, the pure barium hexaferrite sample without any binder has an average density of 4.3 g/cm³ and a porosity of about 13.1%. This reflects a relatively dense material after sintering, though some pores remain. When 5% PVA binder was added, the density dropped noticeably to 3.13 g/cm³, while porosity increased to 18.47%. This decrease in density is likely due to the organic binder evaporating during sintering, which leaves behind voids and tiny pores in the ceramic matrix. At 10% PVA, a similar pattern appeared: density slightly decreased further to 3.07 g/cm³, and porosity remained high at 17.72%. Although there was a small drop in porosity compared to the 5% sample, it still suggests that adding PVA does not significantly reduce porosity overall. This finding is supported by the study conducted by Yanık et al., (2023), which reported that PVA, due to its higher decomposition temperature, promotes pore formation within the material, leading to increased porosity. The evaporation of PVA during heat treatment generates more voids and a less dense structure, thereby enhancing porosity (Wang et al., 2010b; Wang et al., 2023a).

Table 1. Sample density and porosity of barium hexaferrite at different binders (PVA and SR).

Sample	Density (g/cm³)	Porosity (%)
$BaFe_{12}O_{19}$ (Control)	4.3 ± 0,1	13,1 ± 0,1
$BaFe_{12}O_{19}$ + PVA 5%	3,13 ± 0,02	18,47 ± 2,19
$BaFe_{12}O_{19}$ + Silicon Rubber 5%	3,65 ± 0,01	6,95 ± 0,68
$BaFe_{12}O_{19}$ + PVA 10%	3,07 ± 0,03	17,72 ± 0,32
$BaFe_{12}O_{19}$ + Silicon Rubber 10%	3,57 ± 0,02	7,51 ± 0,43

In contrast, samples using silicone rubber showed higher densities—3.65 g/cm³ at 5% concentration and 3.57 g/cm³ at 10%—along with much lower porosities around 7%. This points to a denser, more compact microstructure. The reason lies in the chemical nature of SR; as a cross-linked polymer, it forms a strong and flexible 3D network that helps maintain the green body's density during sintering (Filippova et al., 2023; Liu et al., 2019). Significant differences in porosity, such as 7% versus 18%, have a noticeable effect on both the mechanical and magnetic properties of barium hexaferrite. Higher porosity weakens the material's mechanical strength by increasing the gaps between particles, which also hinders magnetization due to less efficient magnetic domain alignment (Soto-Bernal et al., 2015). On the other hand, SR offers greater elasticity, allowing it to better adapt to thermal stresses, which leads to more even densification. SR samples show a denser microstructure, which is ideal for high-density applications (Kojima et al., 2010; Makhdoom et al., 2021). SR binds barium hexaferrite ceramics better than PVA, making them compact and porous (Chen et al., 2019; Song et al., 2022; Soto-Bernal et al., 2015) . In short, SR is more effective than PVA in increasing density and reducing porosity, resulting in improved particle contact, which enhances mechanical properties like hardness and strength.

This enhanced densification makes SR-bound barium hexaferrite more suitable for advanced structural and functional applications.

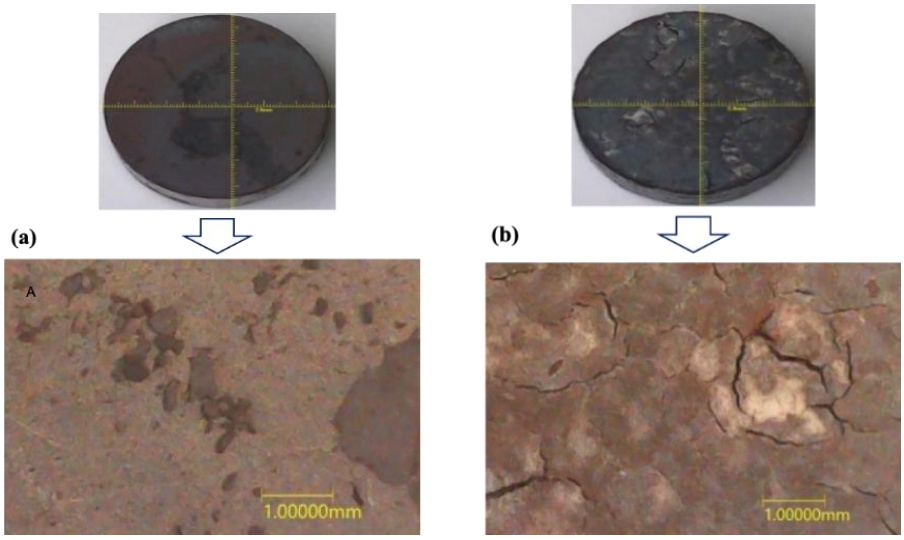

Figure 4. Macrostructure of barium hexaferrite magnet samples prepared with (a) PVA and (b) SR binders.

Figure 4 shows the differences in the surface characteristics of samples using PVA and SR binders. This surface characteristics can be attributed to the chemical properties and bonding efficiency of the binders. The surface of the sample using the PVA binder showed a higher smoothness compared to the surface of a sample that used the SR binder. Microscopic observations reveal that the PVA binder surface appears flatter and more devoid of significant defects (Reddy et al., 2023). Conversely, the sample surface with the SR binder tends to have clearly visible cracks. The thermal tension during the sintering process or the SR binder's less efficient bonding are most likely the cause of this crack. The less effective bonding may be due to the SR binder's less capable chemical properties, which do not optimally unite the material's particles during heating.

3.4 Physical Properties (Shrinkage)

Table 2 shows a comparative analysis revealing significant performance variations of barium hexaferrite between the use of PVA and SR adhesives at concentrations of 5% and 10%. At a concentration of 5%, samples with PVA binder exhibited diameter, thickness, and mass shrinkage of 1.5%, 0.6%, and 7%, respectively. Meanwhile, the sample with the same concentration of SR glue shows a diameter, thickness, and mass shrinkage of 5.4, 3.7, and 7.7%. This suggests that SR glues result in a larger reduction in both diameter and density when compared to PVA adhesives, even though the mass shrinkage is relatively similar. At a concentration of 10%, samples with PVA showed higher shrinkage compared to silicon rubber.

Table 2. Physical properties (shrinkage diameter, thickness, and mass).

Barium hexaferrite + variation of binders	Diameter Shrinkage (%)	Thickness Shrinkage (%)	Mass Shrinkage (%)
PVA 5%	1,5 ± 0,9	0,6 ± 0,1	7 ± 0,9
Silicon Rubber 5%	5,4 ± 0,6	3,7 ± 0,7	7,7 ± 0,9
PVA 10%	2,1 ± 0,3	5,1 ± 4,1	12,2 ± 0,7
Silicon Rubber 10%	5,5 ± 1,4	4,3 ± 0,7	10,4 ± 0,2

Overall, the research results show that PVA adhesives tend to cause greater shrinkage in diameter and thickness compared to SR adhesives, while PVA glues show greater mass shrinkage at a concentration of 10%. Due to the evaporation of absorbed water in its polymer structure, PVA, a water-absorbing hydrophilic polymer, tends to experience significant contraction in applications involving

high temperatures. This makes the material structure of barium hexaferrite less dimensionally stable (Agayev et al., 2022; Ali et al., 2021; Li et al., 2021). In contrast, SR binders exhibit superior thermal properties and chemical stability. SR can withstand high temperatures and extreme environmental conditions, making it more resistant to shrinkage or dimensional deformation (Agayev et al., 2022b; Kaur et al., 2015). These findings provide valuable insights for selecting appropriate binders in applications where precise control over the material's physical dimensions is essential.

3.4 Vickers Hardness Test

Figure 5 displays the results of the Vickers hardness (HV) test on barium hexaferrite samples sintered at 1100 °C. The samples are labeled as PA (PVA 5%), PB (PVA 10%), SA (SR 5%), and SB (SR 10%). The Vickers strength of barium hexaferrite without adhesive is 100.43 HV. The addition of various types of adhesives gives a significant variation in the strength value. With the addition of 5% PVA adhesive, the strength rises to 113,9 HV, while 5% SR increases hardness more substantially to 232.9 HV. Increasing the PVA concentration to 10% further improves hardness to 143.37 HV, whereas 10% SR yields the highest hardness of 438.92 HV.

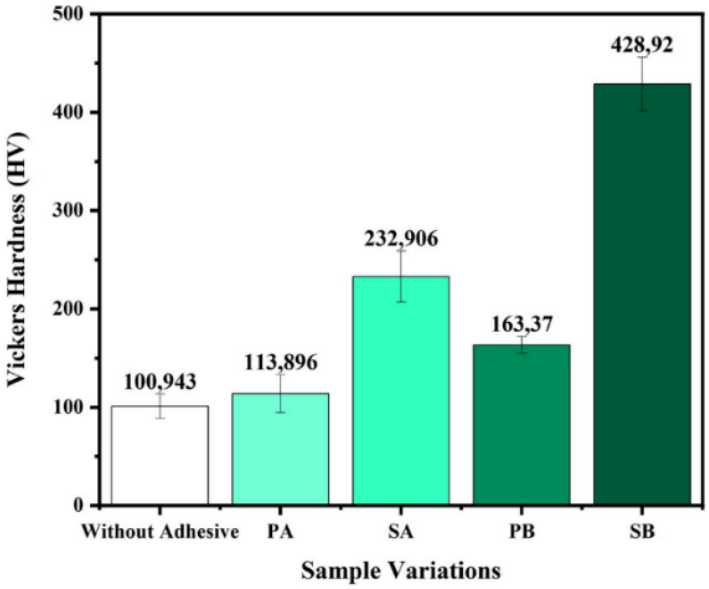

Figure 5. Hardness properties of barium hexaferrite with binder variations (PVA and SR).

As the binder percentage increases, the probability of interparticle bonding also increases, resulting in more dense and harder material. Overall, we conclude that SR binder significantly increases the hardness of barium hexaferrite when compared to PVA. SR adhesives maintain material structure better during and after sintering. This is due to the intrinsic chemical and physical nature of silicone rubber, which forms a resilient, cross-linked polymer network that acts as a robust "binder tissue", effectively locking the hexaferrite particles in place during sintering. This network resists thermal degradation better than PVA, preserving structural integrity and contributing to enhanced mechanical strength.

In contrast, PVA, an organic polymer with a relatively low decomposition temperature, tends to degrade during high-temperature sintering. This degradation leaves behind voids and structural defects, weakening interparticle cohesion and reducing overall mechanical strength (Manglam et al., 2020). The breakdown of PVA during sintering significantly compromises the mechanical performance of the final product. Thus, hardness measurements indicate that SR not only facilitates better densification but also improves the mechanical robustness of barium hexaferrite ceramics due to its chemical stability and elastic polymer network. These findings provide critical guidance for selecting the appropriate type and concentration of binder in applications requiring high-strength magnetic materials.

4. CONCLUSION

The variation in PVA (Polyvinyl Alcohol) and SR (Silicone Rubber) binder concentrations significantly influences the physical, magnetic, and hardness properties of barium hexaferrite sintered at 1100°C. SEM results show an average particle size of approximately 0.7μm, and both SEM and EDX analyses confirm that the milling and sintering process at 1100°C produced barium hexaferrite with the desired structure and composition.

The findings indicate that SR is more effective than PVA in producing denser and less porous barium hexaferrite ceramics. When using SR, there is a larger decrease in the size and thickness of the material compared to PVA at equivalent concentrations. At 10% concentration, PVA shows a greater mass reduction than SR, whereas, at 5%, the mass reduction is similar for both binders. Pure barium hexaferrite, without any binder, exhibits the greatest increase in magnetization after sintering. Adding PVA or SR reduces the enhancement of magnetization, with SR yielding the highest mechanical strength, reaching 438.92 HV. In contrast, barium hexaferrite non-binder shows the lowest strength.

Overall, these results demonstrate that binder type and concentration significantly impact the physical and magnetic properties of barium hexaferrite. SR proves particularly effective at enhancing mechanical strength, while PVA is better at minimizing mass shrinkage and improving magnetization. These insights are valuable for optimizing the performance of magnetic materials in applications that require high strength and improved magnetic properties.

ACKNOWLEDGEMENT

This work is supported by the Institut Teknologi Sumatera (ITERA) through the research scheme of “Madya Hibah penelitian ITERA tahun anggaran 2023 under contract number of 631am/IT9.2.1/PT.01.03/2023.

REFERENCE

An, G.-H., Hwang, T.-Y., Kim, J., Kim, J., Kang, N., Jeon, K.-W., Kang, M., & Choa, Y.-H. (2014). Novel method for low temperature sintering of barium hexaferrite with magnetic easy-axis alignment. *Journal of the European Ceramic Society*, *34*(5), 1227–1233. https://doi.org/10.1016/j.jeurceramsoc.2013.10.027

Banerjee, M., Jain, A., & Mukherjee, G. S. (2019). Microstructural and optical properties of polyvinyl alcohol/manganese chloride composite film. *Polymer Composites*, *40*(S1). https://doi.org/10.1002/pc.25017

Breitwieser, R., Acevedo, U., Ammar, S., & Valenzuela, R. (2017). Ferrite Nanostructures Consolidated by Spark Plasma Sintering (SPS). In *Nanostructured Materials - Fabrication to Applications*. InTech. https://doi.org/10.5772/68017

Cui, J., Ormerod, J., Parker, D., Ott, R., Palasyuk, A., Mccall, S., Paranthaman, M. P., Kesler, M. S., McGuire, M. A., Nlebedim, I. C., Pan, C., & Lograsso, T. (2022). Manufacturing Processes for Permanent Magnets: Part I—Sintering and Casting. *JOM*, *74*(4), 1279–1295. https://doi.org/10.1007/s11837-022-05156-9

Darmawan, L., Manaf, A., Prasetyo, E., Nurjaman, F., Handoko, A. S., Herliana, U., Bahfie, F., & Susanti, D. (2025). The Development of Rare Earth Based Permanent Magnets and Its Relation to the Circular Economy. *Johnson Matthey Technology Review*, *69*(2), 233–246. https://doi.org/10.1595/205651324X17222696085149

El Shater, R. E., El-Ghazzawy, E. H., & El-Nimr, M. K. (2018). Study of the sintering temperature and the sintering time period effects on the structural and magnetic properties of M-type hexaferrite BaFe12O19. *Journal of Alloys and Compounds*, *739*, 327–334. https://doi.org/10.1016/j.jallcom.2017.12.228

Filippova, S. S., Deriabin, K. V., Perevyazko, I., Shamova, O. V., Orlov, D. S., & Islamova, R. M. (2023). Metal- and Peroxide-Free Silicone Rubbers with Antibacterial Properties Obtained at Room Temperature. *ACS Applied Polymer Materials*, *5*(7), 5286–5296. https://doi.org/10.1021/acsapm.3c00697

Ghorbani, Y., Ilankoon, I. M. S. K., Dushyantha, N., & Nwaila, G. T. (2025). Rare earth permanent magnets for the green energy transition: Bottlenecks, current developments and cleaner production solutions. *Resources, Conservation and Recycling*, *212*, 107966. https://doi.org/10.1016/j.resconrec.2024.107966

Gutfleisch, O., Willard, M. A., Brück, E., Chen, C. H., Sankar, S. G., & Liu, J. P. (2011). Magnetic Materials and Devices for the 21st Century: Stronger, Lighter, and More Energy Efficient. *Advanced Materials*, *23*(7), 821–842. https://doi.org/10.1002/adma.201002180

Hassan, S. ul, Hou, L., Kuang, D., & Wang, S. (2024). Carbon based Composite Materials for Microwave Absorption in Low Frequency S and C Band: A Review. *ChemNanoMat*, *10*(12). https://doi.org/10.1002/cnma.202400406

Hirosawa, S., Nishino, M., & Miyashita, S. (2017). Perspectives for high-performance permanent magnets: applications, coercivity, and new materials. *Advances in Natural Sciences: Nanoscience and Nanotechnology*, *8*(1), 013002. https://doi.org/10.1088/2043-6254/aa597c

Idayanti, N., Kristiantoro, T., Septiani, A., & Kartika, I. (2017). Magnetic properties of barium ferrite after milling by high energy milling (hem). *MATEC Web of Conferences*, *101*, 01011. https://doi.org/10.1051/matecconf/201710101011

Idayanti, N., & Manaf, A. (2018). Magnet Nanokomposit Sebagai Magnet Permanen Masa Depan. *Metalurgi*, *1*. www.ejurnalmaterialmetalurgi.com

Islam, R., Vero, K., & Borah, J. P. (2024). Historical overview and recent advances in permanent magnet materials. *Materials Today Communications*, *41*, 110538. https://doi.org/10.1016/j.mtcomm.2024.110538

Kanagesan, S., Hashim, M., Kalaivani, T., Ismail, I., Rodziah, N., Ibrahim, I. R., & Rahman, N. A. (2015). Sintering temperature dependence of optimized microstructure formation of BaFe12O19 using sol–gel method. *Journal of Materials Science: Materials in Electronics*, *26*(3), 1363–1367. https://doi.org/10.1007/s10854-014-2547-1

KOJIMA, T., OORI, S., WATANABE, T., SHIMADA, Y., NORO, S., UEKAWA, N., & KAKEGAWA, K. (2010). Microstructure control of Ce-TZP/Ba ferrite composites using an amorphous precursor of the second phase. *Journal of the Ceramic Society of Japan*, *118*(1381), 823–826. https://doi.org/10.2109/jcersj2.118.823

Koutzarova, T., Kolev, S., Ghelev, Ch., Nedkov, I., Vertruen, B., Cloots, R., Henrist, C., & Zaleski, A. (2013). Differences in the structural and magnetic properties of nanosized barium hexaferrite powders prepared by single and double microemulsion techniques. *Journal of Alloys and Compounds*, *579*, 174–180. https://doi.org/10.1016/j.jallcom.2013.06.049

Liu, Y., Yi, Y., Shao, W., & Shao, Y. (2013). Microstructure and magnetic properties of soft magnetic powder cores of amorphous and nanocrystalline alloys. *Journal of Magnetism and Magnetic Materials*, *330*, 119–133. https://doi.org/10.1016/j.jmmm.2012.10.043

Liu, Y., Zhang, K., Sun, J., Yuan, J., Yang, Z., Gao, C., & Wu, Y. (2019). A Type of Hydrogen Bond Cross-Linked Silicone Rubber with the Thermal-Induced Self-Healing Properties Based on the Nonisocyanate Reaction. *Industrial & Engineering Chemistry Research*, *58*(47), 21452–21458. https://doi.org/10.1021/acs.iecr.9b03953

Madavali, B., Lee, C.-H., Han, J.-G., Kim, D. H., Kim, J. T., Song, G., Lee, J. K., & Hong, S.-J. (2021). Investigation of homogeneity in microstructure and thermoelectric properties at various positions in high-thickness sintered bulks of p-type 20%Bi2Te3–80%Sb2Te3 alloys. *Journal of Materials Science: Materials in Electronics*, *32*(12), 16302–16310. https://doi.org/10.1007/s10854-021-06178-w

Mahmood, S. H., & Bsoul, I. (2012). Hopkinson peak and superparamagnetic effects in $BaFe_{12-x}Ga_xO_{19}$ nanoparticles. *EPJ Web of Conferences*, *29*, 00039. https://doi.org/10.1051/epjconf/20122900039

Makhdoom, A. R., Ranjha, Q. A., Ghori, U.-R., Raza, M. A., Raza, B., Mazhar, M. E., Rao, K. A., Ahmed, F., Asif, S. U., Khan, M. W., & Nisa, M. (2021). Structural and magnetic variations in $Ba_{0.5}Sr_{0.5}Fe_9Ce_1Al_2O_{19}$ hexaferrites at different sintering temperatures. *Physica Scripta*, *96*(12), 125865. https://doi.org/10.1088/1402-4896/ac3d4f

Manglam, M. K., Kumari, S., Mallick, J., & Kar, M. (2021). Crystal structure and magnetic properties study on barium hexaferrite of different average crystallite size. *Applied Physics A: Materials Science and Processing*, *127*(2). https://doi.org/10.1007/s00339-020-04232-8

Manglam, M. K., Kumari, S., Pradhan, L. K., Kumar, S., & Kar, M. (2020). Lattice strain caused magnetism and magnetocrystalline anisotropy in Zn modified barium hexaferrite. *Physica B: Condensed Matter*, *588*, 412200. https://doi.org/10.1016/j.physb.2020.412200

Martínez-Hernando, M.-P., Bolonio, D., Ortega, M. F., Llamas, J. F., & García-Martínez, M.-J. (2023). Material flow analysis and regional greenhouse gas emissions associated to permanent magnets and batteries used in electric vehicles. *Science of The Total Environment*, *904*, 166368. https://doi.org/10.1016/j.scitotenv.2023.166368

Owens, G. J., Singh, R. K., Foroutan, F., Alqaysi, M., Han, C.-M., Mahapatra, C., Kim, H.-W., & Knowles, J. C. (2016). Sol–gel based materials for biomedical applications. *Progress in Materials Science*, *77*, 1–79. https://doi.org/10.1016/j.pmatsci.2015.12.001

Özdemir Yanık, M. C., Demirel, O., Elmadağlı, M., Günay, E., & Aydın, S. (2023). Investigation of glass sintering to improve strength and interfacial interactions in glass-to-AISI 316L metal joints. *International Journal of Applied Glass Science*, *14*(2), 256–267. https://doi.org/10.1111/ijag.16617

P. Singh, V., Kumar, G., Dhiman, P., K. Kotnala, R., Shah, J., M. Batoo, K., & Singh, M. (2014). Structural, Dielectric And Magnetic Properties Of Nanocrystalline BaFe12O19 Hexaferrite Processed Via Sol-gel Technique. *Advanced Materials Letters*, *5*(8), 447–452. https://doi.org/10.5185/amlett.2014.554

Reddy, B. R. S., Ahn, J.-H., Ahn, H.-J., Cho, G.-B., & Cho, K.-K. (2023). Low-Cost and Sustainable Cross-Linked Polyvinyl Alcohol–Tartaric Acid Composite Binder for High-Performance Lithium–Sulfur Batteries. *ACS Applied Energy Materials*, *6*(11), 6327–6337. https://doi.org/10.1021/acsaem.3c00896

Ridwan, R., Mujamilah, M., & Johan, A. (2011). The Semi-Quantitative Study Of Magnetization Process On Milling And Reannealing Of Barium Hexaferrite (BAO.6FE2O3). *Atom Indonesia*, *35*(2). https://doi.org/10.17146/aij.2009.49

Rusianto, T., Waziz Wildan, M., Abraha, K., & Kusmono, K. (2015). Characterizations of Ceramic Magnets from Iron Sand. *International Journal of Technology*, *6*(6), 1017. https://doi.org/10.14716/ijtech.v6i6.1572

Soto-Bernal, J. J., Gonzalez-Mota, R., Rosales-Candelas, I., & Ortiz-Lozano, J. A. (2015). Effects of Static Magnetic Fields on the Physical, Mechanical, and Microstructural Properties of Cement Pastes. *Advances in Materials Science and Engineering*, *2015*, 1–9. https://doi.org/10.1155/2015/934195

Thongsamrit, W., Jantaratana, P., Charoensuk, T., & Sirisathitkul, C. (2022). Paste-Injection of Low-Density Barium Hexaferrite Magnets with Soft Magnetic Iron Phase. *Metals*, *12*(10), 1659. https://doi.org/10.3390/met12101659

Vinnik, D., Tarasova, A., Zherebtsov, D., Gudkova, S., Galimov, D., Zhivulin, V., Trofimov, E., Nemrava, S., Perov, N., Isaenko, L., & Niewa, R. (2017). Magnetic and Structural Properties of Barium Hexaferrite BaFe12O19 from Various Growth Techniques. *Materials*, *10*(6), 578. https://doi.org/10.3390/ma10060578

Wagner, D. V., Kareva, K. V., Zhuravlev, V. A., Dotsenko, O. A., & Minin, R. V. (2023). Investigation of BaFe12O19 Hexaferrites Manufactured by Various Synthesis Methods Using a Developed Pulsed Magnetometer. *Inventions*, *8*(1), 26. https://doi.org/10.3390/inventions8010026

Wahyu Soalfide Sipahutar, & Muljadi. (2021). Pengaruh Waktu Miling terhadap Sifat Mikro Struktur dan Magnet dari NdFeB dengan Proses Wet dan Dry Milling. *Jurnal Teori Dan Aplikasi Fisika*, *09*(01).

Wang, H. Z., He, Q., Wen, G. H., Wang, F., Ding, Z. H., & Yao, B. (2010a). Study of formation mechanism of barium hexaferrite by sintering curve. *Journal of Alloys and Compounds*, *504*(1), 70–75. https://doi.org/10.1016/j.jallcom.2010.05.050

Wang, H. Z., He, Q., Wen, G. H., Wang, F., Ding, Z. H., & Yao, B. (2010b). Study of formation mechanism of barium hexaferrite by sintering curve. *Journal of Alloys and Compounds*, *504*(1), 70–75. https://doi.org/10.1016/j.jallcom.2010.05.050

Wang, X., Wang, B., Wei, S., Wang, Y., & Liang, Y. (2023a). Effect of sintering temperature on the microstructure, magnetic, and microwave absorption properties of M-type barium ferrite nanoparticles prepared by sol–gel method. *Journal of Materials Science: Materials in Electronics*, *34*(12), 1045. https://doi.org/10.1007/s10854-023-10400-2

Wang, X., Wang, B., Wei, S., Wang, Y., & Liang, Y. (2023b). Effect of sintering temperature on the microstructure, magnetic, and microwave absorption properties of M-type barium ferrite nanoparticles prepared by sol–gel method. *Journal of Materials Science: Materials in Electronics*, *34*(12), 1045. https://doi.org/10.1007/s10854-023-10400-2

Zou, J., Zhao, Z., Zhou, X., & Xie, Q. (2023). Effect of Sintering Temperature on the Magnetic Properties of Fe3Mn3Co60.66Si33.34. *Inorganics*, *11*(7), 272. https://doi.org/10.3390/inorganics11070272